Title
Bmi1-Progenitor Cell Ablation Impairs the Angiogenic Response to Myocardial Infarction

Journal
Arteriosclerosis Thrombosis and Vascular Biology, 38(9)

ISSN
1079-5642

Authors
Herrero, Diego
Cañón, Susana
Pelacho, Beatriz
et al.

Publication Date
2018-09-01

DOI
10.1161/atvbaha.118.310778

Peer reviewed

HHS Public Access

Author manuscript

Arterioscler Thromb Vasc Biol. Author manuscript; available in PMC 2019 September 01.

Published in final edited form as:

Arterioscler Thromb Vasc Biol. 2018 September ; 38(9): 2160–2173. doi:10.1161/ATVBAHA.118.310778.

Bmi1-progenitor cell ablation impairs the angiogenic response to myocardial infarction

Diego Herrero[1], **Susana Cañón**[1], **Beatriz Pelacho**[2,3], **María Salvador-Bernáldez**[1], **Susana Aguilar**[1], **Cristina Pogontke**[4], **Rosa María Carmona**[1], **Jesús María Salvador**[1], **Jose María Perez-Pomares**[4], **Ophir David Klein**[5], **Felipe Prósper**[2,3], **Luis Jesús Jimenez-Borreguero**[6], and **Antonio Bernad**[1,*]

[1]Department of Immunology and Oncology, National Center for Biotechnology (CNB-CSIC), 28049 Madrid, Spain

[2]Center for Applied Medical Research (CIMA) Regenerative Medicine Area, University of Navarra, 31080 Pamplona, Spain

[3]IdiSNA, Navarra Institute for Health Research, 31080 Pamplona, Spain

[4]Department of Animal Biology, Faculty of Sciences, Instituto de Investigación Biomédica de Málaga (IBIMA), University of Málaga, 29071 Malaga & BIONAND, Centro Andaluz de Nanomedicina y Biotecnología (Junta de Andalucía, Universidad de Málaga), 29590 Málaga, Spain

[5]Department of Orofacial Sciences and Program in Craniofacial Biology, University of California San Francisco, San Francisco, CA 94143, USA

[6]Cardiovascular Development and Repair Department, National Cardiovascular Research Center (CNIC), 28029 Madrid & Hospital de la Princesa, 28006, Madrid, Spain

Abstract

Objective—Cardiac progenitor cells reside in the heart in adulthood, although their physiological relevance remains unknown. Here we demonstrate that after myocardial infarction, adult Bmi1$^+$ cardiac cells are a key progenitor-like population in cardiac neovascularization during ventricular remodeling.

Approach and Results—These cells, which have a strong *in vivo* differentiation bias, are a mixture of endothelial- and mesenchymal-related cells with *in vitro* spontaneous endothelial cell differentiation capacity. Genetic lineage tracing analysis showed that heart-resident Bmi1$^+$ progenitor cells proliferate after acute myocardial infarction and differentiate to generate *de novo* cardiac vasculature. In a mouse model of induced myocardial infarction, genetic ablation of these cells substantially deteriorated both heart angiogenesis and the ejection fraction, resulting in an ischemic-dilated cardiac phenotype.

[*]**Corresponding author:** Antonio Bernad, Department of Immunology and Oncology, National Center for Biotechnology (CNB-CSIC), Campus de Cantoblanco de la Universidad Autónoma de Madrid, E-28049 Madrid, Spain. abernad@cnb.csic.es; Tel: [+34] 91 585-5424; Fax: [+34] 91 585-4506.

DISCLOSURES

None

Conclusions——These findings imply that endothelial-related Bmi1$^+$ progenitor cells are necessary for injury-induced neovascularization in adult mouse heart, and highlight these cells as a suitable therapeutic target for preventing dysfunctional left ventricular remodeling after injury.

Keywords

Bmi1; cardiac progenitor cell; ischemic dilated cardiomyopathy; endothelial progenitor; angiogenesis

INTRODUCTION

Cardiovascular disease is the main cause of morbidity and mortality in the developed world; acute myocardial infarction (AMI), the most prominent cardiac disease in adults, affects millions of people.[1] During AMI, mechanical and chemical stress induce massive loss of cardiomyocytes and cardiac vasculature, followed by a critical revascularization process and formation of a fibrotic scar.[2] After damage, organized ventricular remodeling is the major determinant of long-term survival.[3] To preserve cardiac function after AMI, the mammalian heart develops a hypertrophic response. In some cases, damage evolves to ischemic dilated phenotype characterized by left ventricular enlargement, that tends to progress to systolic dysfunction and end-stage disease.[4] Despite intensive research to identify genetic mutations involved in the development of inherited cardiomyopathies,[5] only a few studies have focused on the relevance of endogenous adult cell populations in AMI evolution.[6, 7]

Adult cardiac progenitor cells and proliferation of mature cardiac cells are reported to contribute to murine cardiac cell turnover.[8, 9] Cardiac progenitor cells were described more than ten years ago based on c-kit expression.[10] Since then, several adult cardiac progenitor cells have been proposed based on membrane markers (Sca1,[11] Abcg2,[12] Myh6,[13] and PDGFRα[14]) or transcription factors (Isl1,[15] Gli1[6] and Bmi1[16]), although their contribution to *de novo* cardiac cell turnover is relatively slow in homeostasis. These cardiac progenitor subsets might represent transient physiological states of a single cell population.

The importance of these adult cardiac cell populations was nonetheless always based on lineage tracing experiments.[17] In contrast to other organs such as intestine,[18] bone marrow,[19] and lung,[20] the physiological relevance of cardiac progenitor cells has not been demonstrated functionally by their elimination from the adult heart. Only Gli1$^+$ fibroblast progenitor cells have been described as detrimental in ventricular remodeling after AMI.[6] We previously identified that *Bmi1* is preferentially expressed by a subpopulation of Sca1$^+$ cardiac progenitor cells in murine adult heart (≈5% of Sca1$^+$ cells), and Sca1$^+$Bmi1$^+$ cells are able to differentiate to the three main cardiac lineages.[16] The physiological relevance of these progenitor cells nonetheless remains undefined. Here, our results indicate that Sca1$^+$Bmi1$^+$ cardiac cells (hereafter Bmi1$^+$ cells) have a mainly endothelial-related phenotype and contribute markedly to *de novo* cardiac vasculature in post-AMI revascularization. Resident Bmi1$^+$ cardiac progenitor cells are necessary for natural ventricular remodeling after AMI; their depletion induces a deficient angiogenic response and increased scar size, leading to a ischemic-dilated cardiac phenotype in mice.

MATERIAL AND METHODS

The data that support the findings of this study are available from the corresponding author upon reasonable request.

Transgenic mice and tamoxifen administration

Transgenic mice were *Bmi1*$^{CreERT/+}$ (Ref. 21), *Bmi1*$^{GFP/+}$ (Ref. 22), *Rosa26*$^{DTA/+}$ (Ref. 23), *Rosa26*$^{YFP/+}$, *Rosa26*$^{Tomato/+}$ (Ai9) and *β-actin*$^{GFP/+}$ (all from Jackson Laboratory), all on the C57BL/6 background. The full description of transgenic mouse lines and their application in this study can be consulted in Table I in the online-only Data Supplement. Tamoxifen (Tx) was dissolved in corn oil (Sigma); mice received Tx (i.p.) every 24 h for three consecutive days (225 μg/g body weight daily), or once (7.5 μg/g body weight) for low Tx induction. Since preliminary analysis showed no differences between male and female mice, all experiments were carried out in males and females, as recommended by the US National Institutes of Health.[24] Animal studies were approved by the CNB-CSIC Ethics Committee and by the Division of Animal Protection of the Comunidad de Madrid (PA 56/11, PROEX 048/16). All animal procedures conformed to EU Directive 2010/63EU and Recommendation 2007/526/EC regarding the protection of animals used for experimental and other scientific purposes, enforced in Spanish law under Real Decreto 1201/2005.

Acute myocardial infarction and 5-fluorouracil (5-FU) treatment

Mice were anesthetized with 4% sevoflurane, intubated, and ventilated with a 50% air:oxygen mixture using a positive-pressure respirator (Minivent 845, Harvard; 160 strokes/min, 250 μl tidal volume). A left thoracotomy was performed via the fourth intercostal space and the lungs retracted to expose the heart. After opening the pericardium, we ligated the left anterior descending coronary artery with 7–0 silk suture approximately ~2 mm below the edge of the left atrial appendage. Ligation was considered successful when the anterior wall of the left ventricle became pale. The lungs were inflated by increasing positive end-expiratory pressure and the thoracotomy site closed in layers with 6–0 suture. Mice were maintained on a 37°C-heating pad until recovery and for 2 h after surgery. Another group of mice underwent sham ligation, with a similar surgical procedure without tightening the suture around the coronary artery.

To induce bone marrow aplasia, 5-fluorouracil (5-FU; 50 mg/kg body weight; Sigma) was administered (i.v.) and hearts were infarcted four days after drug treatment.

Human heart samples

Human cardiac biopsies were obtained from patients who underwent open-chest surgery, usually for valve replacement. Starting material was obtained from the right atrium appendage, which is routinely removed to place the cannula for extracorporeal circulation. Tissue samples were minced (<1 mm^3 pieces) and treated with collagenase type 2 (Worthington Biochemical; 3 cycles, 30 min each) to obtain a cell suspension. Cardiomyocytes were removed by centrifugation and filtration using 40 μm cell strainers. Human c-Kit$^+$ and c-Kit$^-$ non-myocyte cells were purified from three human myocardial samples by CD45 depletion, followed by c-Kit immunoselection as described,[25] and

expanded for two passages for characterization. Procedures were approved by the hospital ethical committees (Hospital Universitario Gregorio Marañón, Madrid, Spain) with appropriate patient informed consents. All methods were carried out in accordance with current guidelines and regulations (RD 9/2014 and Orden SSI/2057/2014, which transpose the European Commission Directive 2012/39/UE). Cells were maintained and expanded in the growth conditions used for the CAREMI clinical trial (EudraCT 2013–001358-81).[26]

Echocardiography

Mice were anesthetized by isoflurane:oxygen inhalation (1.25:98.75%), and echocardiography performed with a 30-MHz transthoracic echocardiography probe. Images were obtained with the Vevo 2100 micro-ultrasound imaging system (VisualSonics, Toronto, Canada). Measurements of left parasternal long and short axes and M-mode images (left parasternal short axis) were obtained at a heart rate of 500–550 bpm. Left ventricle (LV) end-diastolic diameter (LVEDD), LV end-systolic diameter (LVESD) and wall thickness were measured from M-mode tracings, and the mean of three consecutive cardiac cycles is reported. The LV fractional shortening percentage was calculated as ([LVEDD - LVESD]/LVEDD) × 100. For image acquisition, we used a combination of volume coil/surface coil to enhance signal-to-noise ratio formed by a 72-mm inner diameter quadrature birdcage TX coil (Rapid Biomedical, Rimpar, Germany) and an actively detuning 30-mm flexible customized surface RX coil (Neos Biotec, Pamplona, Spain). Following a tripilot gradient-echo image, a gradient-echo sequence without gating was used to acquire oblique coronal and axial slices. From these images, we determined interventricular septum, LV posterior wall thicknesses, and LV corrected mass; the short-axis M-mode quantification was chosen as most representative. Function was estimated from the ejection fraction and fractional shortening obtained from M-mode views. All procedures were performed blind by two echocardiography experts. For ejection fraction measurements, a long- or short-axis view of the heart was selected to obtain an M-mode registration in a line perpendicular to the LV septum and posterior wall at the level of the mitral chordae tendineae.

For echocardiographic analysis of infarct size 5 days after infarction, regional LV function was evaluated in the parasternal long-axis view. The LV wall was subdivided into 13 segments (basal, mid, and apical from the anterior, posterior, lateral and septal walls, as well as the apex). Each segment was scored in a blind manner by an independent evaluator, based on motion and systolic thickening, according to American Society of Echocardiography guidelines (1, normal or hyperkinetic; 2, hypokinetic; 3, akinetic, negligible thickening; 4, dyskinetic, paradoxical systolic motion; and 5, aneurysmal, diastolic deformation).[27] The number of dysfunctional segments was quantified, and the total score representing the sum of the score of the 13 individual segments was calculated for each heart.[28] At 5 days after infarction, hearts with a score ≤3 with a mild infarction were discarded from the study.

Histology and immunohistochemical analyses

For histological analysis, hearts and small intestines were fixed in 4% paraformaldehyde (PFA; overnight, 4°C), dehydrated and paraffin-embedded for preparation of 10-μm histological sections. Rehydrated slides were stained with Masson’s trichrome. For immunohistochemistry, hearts and small intestines were fixed in 4% PFA as above and

cryopreserved in 30% saccharose, frozen in OCT compound, and sectioned in 8-μm sections on a cryostat. Heart immunohistochemistry and immunocytochemistry have been described.[16] Primary antibodies are shown in Table II in the online-only Data Supplement. A TUNEL assay kit (Roche) was used for histochemical detection of apoptotic cells in heart sections. For histological quantification, at least 30 representative transverse heart or small intestine sections from ventricles and atria were used. Surface areas were quantified by acquiring random images (200x) and calculating the number of stained surfaces per total surface, using ImageJ software (US National Institutes of Health). For $Bmi1^+$ cell detection at 5 days post-low Tx induction, we measured the number and distance of $Bmi1^+$ cells in two ventricular serial histological areas (8 μm x 40 sections) in upper and lower ventricle parts ($n = 3$); we defined a groups of cells as located within a 100 μm radius, considering each histological area as a three-dimensional structure. Images were captured with a Zeiss LSM 700 or Leica TCS SP5 with fixed settings based on negative controls (isotype controls). Processing, including pseudocolor assignment and changes in brightness, was applied uniformly to the entire image to equalize the appearance of multiple panels in a single figure.

Adult cardiomyocyte and non-myocyte cell isolation and cell culture

Non-myocyte cells and cardiomyocytes were obtained by the Langendorff method using retrograde perfusion through the aorta. The heart was removed rapidly and retrograde-perfused under constant pressure (60 mm Hg; 37°C, 8 min) in Ca^{2+}-free buffer (113 mM NaCl, 4.7 mM KCl, 1.2 mM $MgSO_4$, 5.5 mM glucose, 0.6 mM KH_2PO_4, 0.6 mM Na_2HPO_4, 12 mM $NaHCO_3$, 10 mM $KHCO_3$, 10 mM Hepes, 10 mM 2,3-butanedione monoxime, and 30 mM taurine). Digestion was initiated by adding a mixture of recombinant enzymes (0.2 mg/ml Liberase Blendzyme (Roche), 0.14 mg/ml trypsin (ThermoFisher), and 12.5 μM $CaCl_2$ to the perfusion solution). When the heart became swollen (10 min), it was removed and gently teased into small pieces with fine forceps in the enzyme solution. Heart tissue was further dissociated mechanically using 2, 1.5, and 1 mm-diameter pipettes until all large tissue pieces were dispersed. The digestion buffer was neutralized with stopping buffer (10% fetal bovine serum (FBS), 12.5 μM $CaCl_2$). Cardiomyocytes were pelleted by gravity (7 times, 30 min each), the supernatant contains non-myocyte cardiac cells.[16]

Bone marrow cell populations

For bone marrow cell analyses, femurs were removed from mice and bone marrow extracted by complete flushing with PBS in sterile conditions. Bone marrow populations were defined as hematopoietic progenitors ($CD34^+$), pre/pro-B (IgM^-B220^{low}), immature B (IgM^+B220^{low}), lymphocyte B (IgM^+B220^{high}), lymphocyte T-CD4 ($TCRb^+CD4^+$), lymphocyte T-CD8 ($TCRb^+CD8^+$), NK-T ($TCRb^+CD4^-CD8^-$), myeloid immature ($CD11b^{low}Gr1^{high}$), myeloid progenitor + monocytes ($CD11b^{low}Gr1^{low}$), granulocytes ($CD11b^{high}Gr1^{high}$), and NK cells ($CD11b^{low}Gr1^-$). Antibodies are shown in Table II in the online-only Data Supplement.

In vitro cell culture

$Sca1^+Bmi1^+CD31^+CD45^-$ and $Sca1^+Bmi1^+PDGFR\alpha^+CD45^-$ cells were sorted (BC GALIOS) from non-myocyte heart fractions and cultured in Iscove's modified Dulbecco's medium (IMDM, Invitrogen) containing 10% fetal bovine serum (Gibco), 100 IU/ml

penicillin, 100 mg/ml streptomycin and 2 mM L-glutamine (all from Invitrogen), 10^3 units ESGRO Supplement (Millipore), 10 ng/ml EGF (epidermal growth factor; Sigma) and 20 ng/ml FGF (fibroblast growth factor; Peprotech) (37°C, 3% O_2, 5% CO_2). Primary cardiac endothelial cells ($CD31^+$) were obtained by immunomagnetic separation (CD31 MicroBeads, Miltenyi) and cultured in VascuLife VEGF Endothelial Medium Complete Kit (Lifeline Cell Technology) (37°C, 21% O_2, 5% CO_2). Primary cardiac cells were used for the experiments at passage ≤ 9.

Matrigel tube formation assay

Matrigel tube formation assay was developed and quantified as detailed.[29]

Cumulative population doubling

Cells were passaged as they reached 80% confluence. Cumulative population doubling at each passage was calculated from the cell count with the equation $N_H / N_I = 2^X$, where N_I is inoculum number, N_H is cell harvest number, and X is population doublings. The population doublings were added to yield cumulative population doubling. Replicative senescence is defined as X < 1 for 2 weeks.

Flow cytometry

For flow cytometry analysis, hearts were digested by the Langendorff method and non-myocyte-enriched fractions analyzed with a Beckman Coulter Moflow XDP cell sorter, and Beckman Coulter GALLIOS Analyzer and BD FACSCanto II cytometers. FlowJo vX1 (TreeStar) software was used for data analysis.

Western blot

For Western blot, cells and tissues were lysed (45 min, 4°C) in radioimmunoprecipitation assay buffer (RIPA; Sigma-Aldrich), with addition of cOmplete, EDTA-free Protease Inhibitor Cocktail (Roche). Proteins were quantitated using the Infinite m200 (Tecan). Lysates were size-fractionated by SDS-PAGE, transferred to Hybond ECL nitrocellulose membranes (GE Healthcare), probed with indicated antibodies (Table II in the online-only Data Supplement), and analyzed by enhanced chemiluminescence (GE Healthcare).

RT-qPCR analysis

RNA was purified using the Cells-to-CT kit (Ambion, Thermo). Complementary DNA was obtained by reverse transcription with the High Capacity cDNA Reverse Transcription Kit (Applied Biosystems). cDNAs were analyzed by real-time PCR using the Power SYBR Green PCR Master Mix (Applied Biosystems). Amplification, detection and data analysis were carried out with an ABI PRISM 7900HT Sequence Detection System and normalized to *GusB* and *Gapdh* expression. Changes in mRNA expression are noted as *x*-fold change relative to the control. qPCR primers are listed in Table II in the online-only Data Supplement.

Statistical analysis

Statistical analyses were performed with GraphPad Prism 6.01. Data were subjected to the Shapiro-Wilk test for normality and F test for equality of variances. For two groups, those that passed normality and equal variance tests were analyzed by the Student's t-test (2-tailed, unpaired) and those that failed normality and equal variance tests were analyzed by non-parametric Mann-Whitney rank sum test. For multiple groups, data that passed normality and equal variance tests were analyzed by one-way ANOVA with Tukey's post-hoc test and those data that failed normality and equal variance tests were analyzed by the Kruskal-Wallis ANOVA with Dunn's multiple comparisons test. To analyze cell distributions, non-parametric two-sample Kolmogorov-Smirnov test was used. Survival curves were generated by the Kaplan-Meier method, and compared using the log-rank test. A value of $P < 0.05$ was considered significant. All replicates considered are biological replicates.

RESULTS

BMI1 expression identifies an endothelial/mesenchymal-related population of non-myocyte cells in adult mouse heart

We used $Bmi1^{GFP/+}$ knock-in mice[22] to analyze *Bmi1* expression in heart compared to constitutive GFP (green fluorescent protein) expression in β-$actin^{GFP/+}$ mice. Comparative FACS (fluorescence-activated cell sorting) analyses showed that in adult heart, *Bmi1* expression was restricted to a subpopulation of non-myocyte cells (Figure 1A). Whereas the fluorescence intensity in GFP^+ non-myocyte cells resembled that of constitutive expression, FACS and immunocytochemistry showed no or very low GFP levels in adult cardiomyocytes (Figures 1B and 1C), as confirmed by RT-qPCR (quantitative reverse transcription polymerase chain reaction) (Figure 1D).

To better define the identity of cardiac $Bmi1^+$ cells, we exhaustively characterized $Bmi1^{CreERT/+}R26^{Tomato/+}$ adult heart sections 5 days post-tamoxifen (Tx) induction. Cardiac $Bmi1^+$ cells were negative for the mature endothelial-related surface markers von Willebrand factor (vWF) and VE-cadherin (CDH5; <2%), although the majority of these cells expressed CD31 (85 ± 3%) (Figure 1E). We also assessed expression of several surface markers reported for adult cardiac progenitor cells.[14, 17, 30] $Bmi1^+$ cells were negative for pericyte-related α-smooth muscle actin (αSMA), pericyte/endothelial melanoma cell adhesion molecule (CD146) and fibroblast-related markers CD90 and FSP-1. They were also negative for the mesenchymal-related markers nestin and endoglin (CD105), although 12 ± 2% of $Bmi1^+$ cells expressed platelet-derived growth factor receptor alpha (PDGFRα; XΔ140α) (Figure 1E), which is linked to the clonogenic $Sca1^+$ cardiac progenitor subpopulation.[14] FACS characterization of whole digested heart showed that CD31 and PDGFRα features were mutually exclusive in $Bmi1^+$ cells (Figure 1F). The data show that *Bmi1* expression is linked to a mixture of endothelial- and mesenchymal-related non-myocyte $Sca1^+$ cells in the adult mouse heart.

Cardiac $Bmi1^+$ cells are not a subpopulation of mature endothelial cells

Although endothelial surface markers are associated with various adult progenitor cell populations,[31–34] CD31 has classically been linked to mature endothelial cells. To rule out

the possibility that cardiac Bmi1$^+$ cells were a mature endothelial cell subpopulation, we compared them to endothelial (CD31$^+$) and mesenchymal (PDGFRα) primary cardiac cells. In the heart, Bmi1$^+$ cells were located in a perivascular position, but never in the tunica intima of blood vessels (Figure IA in the online-only Data Supplement). *In vitro* Bmi1$^+$ cells were morphologically more similar to PDGFRα$^+$ than to CD31$^+$ cells (Figure IB in the online-only Data Supplement). RT-qPCR analyses confirmed an mRNA expression profile intermediate between endothelial and mesenchymal cells (Figure IC in the online-only Data Supplement). Compared to the limited expansion potential of CD31$^+$ primary endothelial cells, cardiac Bmi1$^+$ cells showed stable growth over more than 13 passages (Figure ID in the online-only Data Supplement). Finally, matrigel angiogenesis assays confirmed that primary endothelial cells efficiently formed branching structures *in vitro*, in contrast to Bmi1$^+$ progenitor cells (Figures IE and IF in the online-only Data Supplement). Results suggest that Bmi1$^+$ cells are an endothelial-related population, but cannot be considered mature endothelial cells.

Human c-Kit$^+$ cardiac stem cells are not the main source of *BMI1* in human heart

Although recent studies challenge the identity and the multipotent differentiation capacity of c-Kit$^+$ human cardiac progenitor cells,[35, 36] c-Kit$^+$CD45$^-$ cells are the most widely reported human cardiac stem cells.[37] To evaluate whether these cells are the main source of *BMI1*, we measured its expression in c-Kit$^+$CD45$^-$ compared to c-Kit$^-$CD45$^-$ primary cardiac cells (passage 2), both isolated in parallel from the same heart tissue samples and cultured in low oxygen conditions (3% O_2) to preserve *BMI1* expression (Figure IIA in the online-only Data Supplement). As in the case of murine cardiac progenitor cells,[16] *BMI1* levels were downregulated in cell culture compared to fresh heart tissues (Figure IIB in the online-only Data Supplement). Although the differences between c-Kit$^+$ and c-Kit$^-$ cells were not significant, analysis of individual donors showed that c-Kit$^-$ cells always expressed higher *BMI1* levels (Figure IIC in the online-only Data Supplement). Results showed that c-Kit$^+$ cardiac stem cells are not the main source of *BMI1* in adult human heart.

In vivo differentiation assay of murine cardiac Bmi1$^+$ cells in steady state

Various *in vitro* differentiation protocols are used for adult cardiac progenitor cell differentiation, although the artificial conditions of *in vitro* culture might activate differentiation potential not shared by cells *in vivo*.[36, 38, 39] The presence of two major, mutually exclusive Bmi1$^+$ cell subpopulations in murine hearts (CD31$^+$ and PDGFRα$^+$) prompted us to analyze *in vivo* cell dynamics to identify true differentiation potential. At difference from other organs, the heart lacks a defined, physical niche-like structure;[40] to pinpoint differences in differentiation capacity and *in vivo* cell dynamics, we therefore adjusted the Tx dose (7.5 μg/g weight; low-dose) to label disperse cells (>200 μm). At 5 days post-Tx low-dose induction in Bmi1$^{CreERT/+}$R26$^{Tomato/+}$ mice, the majority of Bmi1$^+$ progenitor cells were spaced more than 200 μm apart (96 ± 3%, n = 205 cells, 3 mice), in contrast to the more closely spaced cell distribution after our standard Tx induction (Figure IIIA in the online-only Data Supplement). FACS analysis of triple transgenic Bmi1$^{GFP/CreERT}$R26$^{Tomato/+}$ hearts confirmed the small percentage of labeled cardiac Bmi1$^+$ cells after low-dose Tx induction (1:1000 Bmi1$^+$ cells; ≈100 Bmi1$^+$ cells/heart) (Figure IIIB in the online-only Data Supplement). Bmi1-derived cell group size increased

homogeneously in an age-dependent fashion, which suggested that there were no subpopulation-associated differences in cell dynamics (Figure 2A; Figure IIIC in the online-only Data Supplement).

As for Sca1^{+} cardiac progenitor cells,[11] there were few groups with the three main cardiac cell lineages (endothelial, smooth muscle and cardiomyocyte), although rare examples were found (Figure 2B; Figure IIID in the online-only Data Supplement). Histological analyses at 6 months after low-dose Tx induction showed that groups of Bmi1-derived endothelial or smooth muscle cells were more frequent than cardiomyocyte groups (Figure 2C). Labeling was negligible in vehicle-treated mice (one group of 1–3 cells in two of four mice at 6 months of age). These results suggest that in homeostasis, adult Bmi1^{+} cardiac cells have a strong *in vivo* differentiation bias, with limited multilineage potential.

In vivo genetic ablation of Bmi1^{+} cardiac progenitor cells by Cre-mediated expression of diphtheria toxin A

To ablate Bmi1^{+} progenitor cells and evaluate their *in vivo* relevance in the adult heart, we crossed Tx-inducible Bmi1^{CreERT} mice with an improved mouse line for Cre-induced cell ablation based on diphtheria toxin A (DTA) expression (R26^{DTA}).[23] Bmi1$^{CreERT/+}$R26$^{DTA/+}$ adult hearts were phenotypically and functionally identical to R26$^{DTA/+}$ control hearts, ruling out non-specific CRE activity in the absence of Tx (Figures IVA through IVC in the online-only Data Supplement). To evaluate system ablation efficiency, we generated the triple transgenic Bmi1$^{CreERT/+}$R26$^{YFP/DTA}$ mouse line (Figure 3A). Five days post-Tx induction, >97% of YFP^{+} cells (2.5 ± 0.4% of total non-myocyte cells) were eliminated compared to bigenic Bmi1$^{CreERT/+}$R26$^{YFP/+}$ control mice (Figure 3A). DTA activity was restricted to non-myocyte cells, as TUNEL (terminal deoxynucleotidyl transferase dUTP nick end labeling) assay ruled out Tx-related apoptosis in cardiomyocytes at 1 and 5 days post-Tx treatment (Figure IVD in the online-only Data Supplement). RT-qPCR and Western blot analyses confirmed significantly reduced BMI1 expression only in the non-myocyte cell fraction, which indicates successful ablation of Bmi1^{+} cardiac progenitor cells after Tx induction (Figures 3B and 3C).

Elimination of Bmi1^{+} progenitor cells induces an ischemic-dilated cardiac phenotype after acute myocardial infarction

With the exception of Gli1^{+} fibroblast progenitor cells,[6] the role of cardiac progenitors after myocardial infarction remains elusive. To test whether Bmi1^{+} progenitor cells are necessary after AMI, Bmi1$^{CreERT/+}$R26$^{DTA/+}$ mice were randomized and subjected to coronary artery ligation or sham surgery two weeks post-Tx induction. Vehicle-treated [Bmi1$^{CreERT/+}$R26$^{DTA/+}$(CO)] and Tx-treated R26$^{DTA/+}$ [R26$^{DTA/+}$(Tx)] mice were used as controls (Figure 4A). Five days post-AMI, echocardiography showed functional decline in all mice groups regardless of Tx treatment (Figure 4B), and confirmed a similar degree of heart dysfunction (Figure IVE in the online-only Data Supplement). Two months after damage, echocardiography detected a reduced left ventricular ejection fraction (EF) in Bmi1$^{CreERT/+}$R26$^{DTA/+}$(Tx) hearts compared with controls (Figure 4B). This cardiac dysfunction was sustained over two additional months and affected survival of Bmi1^{+} cell-deficient mice (Figure 4C). At this time, histological analysis of Bmi1^{+} cell-deficient hearts

confirmed differences in cardiac remodeling compared to infarcted controls. The former presented eccentric cardiac hypertrophy (an ischemic-dilated cardiac phenotype) characterized by left ventricular chamber dilatation, thinning of the interseptal wall and reduced EF (Figures 4D and 4E). We found no differences in left ventricular mass as measured by echocardiography or heart/body weight ratio, although we detected a slight increase in myocyte cross-sectional length in Bmi1^{+} cell-deficient hearts (Figure IVF through H in the online-only Data Supplement), possibly linked to an increase in hemodynamic pressure associated with the deficient left ventricular remodeling after AMI.

Prognosis and progression of ischemic damage depend on fibrotic and angiogenic responses after AMI. Deficiencies in these processes affect cardiac remodeling and induce cardiac dysfunction.[41, 42] Quantification of fibrosis in histological sections showed no notable differences between groups (Figures 5A and 5B), although we detected an increase in left ventricular scar size in Bmi1^{+} cell-deficient hearts (Figure 5C). Histological and FACS analyses showed, and RT-qPCR confirmed, that absence of Bmi1^{+} progenitor cells altered the angiogenic response after AMI; mature endothelium was decreased in scar and in remote infarct areas, particularly in small blood vessels (Figures 5D through 5G).

Extra-cardiac cell ablation does not affect cardiac function

Bmi1 is a marker of various adult stem cell populations,[43] and bone marrow (BM) is considered the main organ in crosstalk with the heart.[44] We previously discarded BM origin of Bmi1^{+} cardiac progenitor cells,[16] but it could be possible that Bmi1-cell ablation affected BM-derived cells (CD45^{+}). Tx treatment provoked no differences in the percentage of BM populations, but induced a non-significant decrease in BM cell numbers (Figures VA and VB in the online-only Data Supplement). In the heart, cardiac resident hematopoietic-derived cells (CD45^{+}) were also unaffected (Figures VC and VD in the online-only Data Supplement). To further confirm the lack of a Bmi1-BM cell role in cardiac dysfunction, we used 5-fluorouracil (5-FU) to induce a decrease in BM cell number, similar to the BM cell ablation after Tx induction in bigenic Bmi1$^{CreERT/+}$R26$^{DTA/+}$ mice (Figure VE in the online-only Data Supplement). Echocardiography data showed neither functional nor structural differences in the hearts of PBS- and 5-FU-treated mice two months after AMI; results were confirmed in histological sections at four months after injury (Figures VF and VG in the online-only Data Supplement). At this time, BM cellularity and the BM cell populations remained normal in Bmi1^{+} cell-deficient mice (Figures VH and VI in the online-only Data Supplement). In addition, despite a decrease of Lgr5^{+} intestinal stem cells two days post-Tx treatment, both intestinal stem cell number and crypt-villus architecture in Bmi1$^{CreERT/+}$R26$^{DTA/+}$ mice two weeks post-Tx (AMI time point) were comparable to that of vehicle treated mice (Figures VJ and VK in the online-only Data Supplement). These results rule out the possibility that extra-cardiac effects alters adult Bmi1$^{CreERT/+}$R26$^{DTA/+}$ mouse survival or cardiac function, and confirm that resident Bmi1^{+} cardiac progenitor cells are necessary in post-ischemic angiogenesis.

Conditional ablation of Bmi1^{+} cells does not affect cardiac function in steady state

We also monitored the cardiac function of Bmi1^{+} cell-deficient [Bmi1$^{CreERT/+}$R26$^{DTA/+}$ (Tx-induced)] and control mice [Bmi1$^{CreERT/+}$R26$^{DTA/+}$ (corn oil vehicle-treated)] for one

year in homeostasis. In contrast to AMI, we detected no major differences in conventional echocardiography parameters or in cardiac histology in one-year-old mice (Figures VIA through VID in the online-only Data Supplement). In accordance, we found no reduction in lifespan in Bmi1^{+} cell-deficient mice (Figure VIE in the online-only Data Supplement). We analyzed adult cell plasticity[45] to test whether the absence of phenotype in Bmi1^{+} cell-deficient hearts was at least in part linked to recovery of Bmi1^{+} cardiac cell population in homeostasis. Lineage tracing analysis at four months post-Tx of rare surviving Bmi1^{+} progenitor cells in trigenic Bmi1$^{CreERT/+}$R26$^{YFP/DTA}$(Tx) mice showed a relative increase in their contribution to cardiac cell progeny compared to bigenic Bmi1$^{CreERT/+}$R26$^{YFP/+}$ control mice (Figures VIIA through VIIC in the online-only Data Supplement). In addition, RT-qPCR and Western blot analyses showed no differences in BMI1 levels between Tx- and CO-treated mice four months post-ablation in contrast to infarcted mice (Figures VIID through VIIF in the online-only Data Supplement). The results suggest that, in homeostasis, Sca1^{+}Bmi1^{+} cardiac cells are not essential for cardiac function and that the heart could has compensatory mechanisms to replenish Sca1^{+}Bmi1^{+} cardiac progenitor cells.

Bmi1^{+} cardiac progenitor cells are a source of endothelial cells after acute myocardial infarction

We induced lineage tracing in Bmi1$^{CreERT/+}$R26$^{YFP/+}$ mice to analyze the real contribution of Bmi1^{+} progenitor cells to cardiac progeny after AMI. To exclude the possibility that residual Tx induces CRE activity in Bmi1^{+} cells following injury, hearts were infarcted 2 weeks post-Tx induction, a period sufficient to ensure its clearance.[46] We also ruled out an AMI-dependent BMI1 upregulation (Figure VIIG in the online-only Data Supplement). Although we confirmed an increase in Bmi1-derived cardiomyocytes in remote areas at 4 months after AMI[47] (Figure VIIH in the online-only Data Supplement), histological and FACS analyses highlighted a relatively large proportion of Bmi1-derived non-myocyte cells (Figures 6A and 6B). Despite 4 months after damage we detected a small percentage of cardiac fibroblasts (<8%) derived from Bmi1^{+} progenitor cells (Figure VIIi in the online-only Data Supplement), we found a striking increase in mature Bmi1-derived endothelial cells (up to 6-fold) (Figure 6C). To confirm the endothelial differentiation potential of Bmi1^{+} cardiac cells, we isolated and cultured Bmi1^{+}CD31^{+} and Bmi1^{+}PDGFRα^{+} primary cells from adult Bmi1$^{CreERT/+}$R26$^{YFP/+}$ mice. Two weeks after cells reached confluence, we observed spontaneous formation of microvascular networks *in vitro*. Compared to Bmi1^{+}PDGFRα^{+} cells Bmi1^{+}CD31^{+} cardiac cells nonetheless produced a higher percentage and larger-sized endothelial-related structures (Figure VIIJ in the online-only Data Supplement).

De novo formation of microvessels is essential for long-term ventricular remodeling after AMI.[41] To evaluate this angiogenic response, we used FACS to quantify *in vivo* endothelial cell dynamics. Three days after AMI, endothelial cells decreased acutely, probably due to the ischemic process. Revascularization began several days after infarction and was complete at two months after AMI (Figure 6D). To analyze the dynamic of Bmi1^{+} cardiac progenitor cells during this revascularization, we also used FACS to trace Bmi1-derived cells from Bmi1$^{CreERT/+}$R26$^{YFP/+}$ mice. We confirmed a significant contribution of these cells to the angiogenic response, which was especially notable from 2 weeks to 2 months after AMI

(Figure 6E). Histological analysis showed Bmi1-derived endothelial cells in infarcted and remote areas, contributing to arterioles in the myocardium and to veins in the subepicardium (Figures 6C and 6F). The results suggest that at four months after damage, Bmi1$^+$ progenitor cells are a relevant source of cardiac endothelial cells, and contribute up to 20% of total endothelial cells in the infarcted heart.

DISCUSSION

Although knowledge of the effect of gene mutations in cardiac disease development is growing rapidly,[5] the role of distinct adult cardiac progenitor cell populations after acute myocardial infarction (AMI) remains poorly understood. Here we show that after AMI, murine cardiac progenitor-like Sca1$^+$Bmi1$^+$ cells[16, 47] are necessary for the angiogenic response and that their absence induces ischemic-dilated cardiac phenotype.

Polycomb-related BMI1 protein is necessary for the maintenance of several adult stem cell populations, mainly through its capacity to inhibit senescence-related genes and to regulate mitochondrial function.[48, 49] In-depth analysis of how BMI1 acts has nonetheless allowed description of specific tissue-related functions. In mesenchymal cells, BMI1 inhibits the expression of key chemokines from the senescence-associated secretory phenotype.[50] In muscle satellite cells, BMI1 enhances progenitor cell protection through metallothionein 1 upregulation.[51] In the heart, recent observations indicate that BMI1 represses a cardiogenic differentiation program,[52, 53] thus identifying cardiac progenitor-like cells.[16] In the majority of tissues, however, high BMI1 expression defines a mixture of progenitor cells and in some cases, Bmi1$^+$ cells are not essential for tissue homeostasis.[54–56] The characteristics and physiological role of Bmi1$^+$ progenitor cells in the adult heart remain unexplored.

Our results showed that in murine adult heart, Bmi1$^+$ cells are a Sca1$^+$ heterogeneous mixture of endothelial- and mesenchymal-related non-myocyte cells. Expression of the endothelial-related CD31 protein in progenitor cells is not uncommon, as endothelial and progenitor cells are linked in several organs during development, and even in adulthood.[33, 57, 58] Proliferation capacity, the mRNA expression profile, and the matrigel angiogenesis assay clearly indicated that cardiac Bmi1$^+$ cells are not mature endothelial cells. An *in vivo* differentiation assay with a very low dose of Tx showed that, after chase, the majority of Bmi1-derived cell groups were composed of only one or two mature cell types. The absence of a direct relationship between group size and number of cardiac cell types might be explained by the more rapid proliferation of endothelial and myofibroblast cells compared to cardiomyocytes,[59] and/or by short-term progenitor identity of the majority of Bmi1$^+$ cells. Since most studies describe limited multipotency in adult cardiac progenitor cells,[11, 36] it is possible that like other transcription factors, BMI1 expression defines a progenitor-like state of several cell populations in the heart.[60, 61] In the human heart, *BMI1* measurement suggests that c-Kit$^+$ cardiac stem cells[10] are not the main *BMI1* source, whose identification requires additional study.

To evaluate the functional importance of Sca1$^+$Bmi1$^+$ cells in murine hearts, we used a conditional Cre-mediated cell ablation system.[23] The Rosa26^{DTA} allele allowed high efficiency removal of Bmi1$^+$ cells labeled in the Rosa26^{YFP} reporter allele (≈3%of non-

myocyte cells). CRE deletion efficiency was analogous in both Rosa26 alleles, probably due to the similar size of the deletion fragments and locus accessibility.[62] One strength of this DTA cellular ablation system is that it allows analysis of cardiac cell dynamics in $Bmi1^+$ cell-deficient hearts considering cardiac cell plasticity;[45] we thus provide a physiological description of the importance of $Bmi1^+$ cardiac progenitor cells.

In contrast to our prediction, Bmi1-progenitor cell ablation in homeostasis did not affect cardiac function or mouse lifespan. In homeostasis, BMI1 expression levels were recovered after several months, accompanied by a relative increase in the contribution of $Bmi1^+$ cells that escaped ablation to cardiac cell progeny, suggesting cardiac cell plasticity.[45] The low adult cardiac cell turnover[59] together with the permissive environment for cell plasticity in homeostasis and the lack of ischemia-mediated cell activation of $Bmi1^+$ cardiac progenitors[47] may explain the absence of cardiac dysfunction in $Bmi1^+$ cell-deficient hearts in homeostasis.

Echocardiography and histological analyses showed that after AMI, nonetheless, $Bmi1^+$ cardiac progenitor cells became necessary for correct ventricular remodeling and cardiac function. Following infarction, the loss of cardiomyocytes and vasculature, accompanied by formation of a fibrotic scar, induces cardiac remodeling.[2] In some cases, however, ischemic damage evolves to eccentric hypertrophy (ischemic-dilated phenotype), characterized by an enlarged left ventricular chamber and thinning of the interventricular septum, in which myocytes typically lengthen; these factors lead to reduced cardiac function.[63] Histological analysis at four months after AMI showed that $Bmi1^+$ cell-deficient hearts developed eccentric hypertrophy compared to control hearts. The cellular cause of this pathological remodeling was probably deficient angiogenesis and increased scar size. The absence of increased fibrosis and the fact that disruption of the angiogenic process can increase scar size[64–66] nonetheless suggest that the cardiac phenotype in $Bmi1^+$ cell-deficient hearts is closely linked to impaired injury-induced angiogenesis.

Endothelial cell subpopulations are able to differentiate into cardiomyocytes, pericytes, and fibroblasts in the adult mouse heart.[30–32] Although endothelial cells make up the cardiac population with highest cell turnover,[59] the source of these cells in adult mice is not clear. Several authors describe an important role for bone marrow-derived circulating endothelial progenitor cells.[67] The mesenchymal-to-endothelial transition is also reported to contribute to substantial numbers of endothelial cells after AMI;[68] a recent study using several genetic-tracing studies nonetheless challenged these conclusions, and suggests that only preexisting endothelial cells and/or endothelial-related progenitor cells contribute to neovascularization after injury.[69] Our results showed that $Sca1^+Bmi1^+$ cells are a relevant population during post-damage angiogenesis, and two months after AMI contribute up to 20% of total cardiac endothelial cells. Of these $Sca1^+Bmi1^+$ cells, the powerful spontaneous endothelial differentiation capacity of $Sca1^+Bmi1^+CD31^+$ compared to $Sca1^+Bmi1^+PDGFR\alpha^+$ cells *in vitro* suggests that $Sca1^+Bmi1^+CD31^+$ cells are the endothelial-related progenitor cell population. The similarity of *in vivo* cell dynamics and the potential of $Sca1^+Bmi1^+PDGFR\alpha^+$ cells to *in vitro* endothelial differentiation, nonetheless stymied our effort to clearly rule out the $PDGFR\alpha^+$ subpopulation.

Depletion of $Bmi1^+$ progenitor cells had no effect on cardiac function in homeostasis. Ablation before injury would nonetheless lead to deficient angiogenesis, giving rise to dysfunctional ventricular remodeling and cardiac failure. Our findings suggest that stimulation of endogenous $Sca1^+Bmi1^+$ cardiac progenitor cells in the infarcted myocardium would help counteract the pathological ventricular remodeling by sustaining injury-induced neovascularization.

Supplementary Material

Refer to Web version on PubMed Central for supplementary material.

ACKNOWLEDGEMENTS

DH conceived, performed and designed experiments, developed the project, contributed ideas and wrote the manuscript. SC, BP and MSB performed and designed experiments. CP, RMC and SA performed experiments. JMP-P, ODK, FP, JMS, and LJJ-B co-supervised specific experiments. AB conceived and developed the project, designed experiments, interpreted results and wrote the manuscript. All authors read and approved the final manuscript.

We thank MC Moreno and S Escudero for the sorting strategy, S Montalbán and O Sánchez for assistance with histology, L Flores and AV Alonso for echocardiography analyses, I Sánchez and L Domínguez for surgical infarcts, S Méndez-Ferrer for the $Rosa26^{DTA/+}$ mouse line, M Torres, I Flores and N Fonseca-Balvís for valuable discussion, and C Mark for editorial assistance.

SOURCES OF FUNDING

DH is an FPI predoctoral fellow of the Spanish Ministry of Economy and Competitiveness. This study was supported by grants to AB from the Ministry of Economy and Competitiveness (MINECO/FEDER) (SAF2015–70882-R), Comunidad Autónoma de Madrid (S2011/BMD-2420), Instituto de Salud Carlos III (ISCIII) (RETICS-RD12/0018) and the European Commission (HEALTH-2009_242038), to JMP-P from the MINECO (BFU2015–65783-R) and ISCIII (RD16/0011/0030), to ODK from the National Institute of Dental and Craniofacial Research (R35-DE026602), and to BP from FEDER (ISCIII: PI16/00129 and CPII15/00017).

ABBREVIATIONS

AMI	Acute myocardial infarction
Sca1	Stem cell antigen-1 (Ly-6A/E)
Bmi1	B lymphoma Mo-MLV insertion region 1 homolog (PCGF4)
c-Kit	A type III receptor tyrosine kinase (CD117)
DTA	Diphtheria toxin A
Tx	Tamoxifen
CreERT	Recombinase to induce specific temporal CRE activity by tamoxifen

REFERENCES

1. Benjamin EJ, Blaha MJ, Chiuve SE, et al. Heart disease and stroke statistics-2017 update: A report from the american heart association. Circulation. 2017;135:146–603
2. French BA, Kramer CM. Mechanisms of post-infarct left ventricular remodeling. Drug Discov Today Dis Mech. 2007;4:185–196 [PubMed: 18690295]

3. White HD, Norris RM, Brown MA, Brandt PW, Whitlock RM, Wild CJ. Left ventricular end-systolic volume as the major determinant of survival after recovery from myocardial infarction. Circulation. 1987;76:44–51 [PubMed: 3594774]
4. Hershberger RE, Morales A, Siegfried JD. Clinical and genetic issues in dilated cardiomyopathy: A review for genetics professionals. Genet Med. 2010;12:655–667 [PubMed: 20864896]
5. Watkins H, Ashrafian H, Redwood C. Inherited cardiomyopathies. N Engl J Med. 2011;364:1643–1656 [PubMed: 21524215]
6. Kramann R, Schneider RK, DiRocco DP, Machado F, Fleig S, Bondzie PA, Henderson JM, Ebert BL, Humphreys BD. Perivascular Gli1^{+} progenitors are key contributors to injury-induced organ fibrosis. Cell Stem Cell. 2015;16:51–66 [PubMed: 25465115]
7. Ruiz-Villalba A, Simón AM, Pogontke C, Castillo MI, Abizanda G, Pelacho B, Sánchez-Domínguez R, Segovia JC, Prósper F, Pérez-Pomares JM. Interacting resident epicardium-derived fibroblasts and recruited bone marrow cells form myocardial infarction scar. J Am Coll Cardiol. 2015;65:2057–2066 [PubMed: 25975467]
8. Senyo SE, Steinhauser ML, Pizzimenti CL, Yang VK, Cai L, Wang M, Wu TD, Guerquin-Kern JL, Lechene CP, Lee RT. Mammalian heart renewal by pre-existing cardiomyocytes. Nature. 2013;493:433–436 [PubMed: 23222518]
9. Nakada Y, Canseco DC, Thet S, et al. Hypoxia induces heart regeneration in adult mice. Nature. 2016;541:222–227 [PubMed: 27798600]
10. Beltrami AP, Barlucchi L, Torella D, Baker M, Limana F, Chimenti S, Kasahara H, Rota M, Musso E, Urbanek K, Leri A, Kajstura J, Nadal-Ginard B, Anversa P. Adult cardiac stem cells are multipotent and support myocardial regeneration. Cell. 2003;114:763–776 [PubMed: 14505575]
11. Uchida S, De Gaspari P, Kostin S, Jenniches K, Kilic A, Izumiya Y, Shiojima I, Grosse Kreymborg K, Renz H, Walsh K, Braun T. Sca1-derived cells are a source of myocardial renewal in the murine adult heart. Stem Cell Reports. 2013;1:397–410 [PubMed: 24286028]
12. Maher TJ, Ren Y, Li Q, Braunlin E, Garry MG, Sorrentino BP, Martin CM. ATP-binding cassette transporter Abcg2 lineage contributes to the cardiac vasculature after oxidative stress. Am J Physiol Heart Circ Physiol. 2014;306:1610–1618
13. Malliaras K, Ibrahim A, Tseliou E, Liu W, Sun B, Middleton RC, Seinfeld J, Wang L, Sharifi BG, Marbán E. Stimulation of endogenous cardioblasts by exogenous cell therapy after myocardial infarction. EMBO Mol Med. 2014;6:760–777 [PubMed: 24797668]
14. Noseda M, Harada M, McSweeney S, et al. PDGFRα demarcates the cardiogenic clonogenic Sca1^{+} stem/progenitor cell in adult murine myocardium. Nat Commun. 2015;6:6930 [PubMed: 25980517]
15. Moretti A, Caron L, Nakano A, Lam JT, Bernshausen A, Chen Y, Qyang Y, Bu L, Sasaki M, Martin-Puig S, Sun Y, Evans SM, Laugwitz KL, Chien KR. Multipotent embryonic Isl1^{+} progenitor cells lead to cardiac, smooth muscle, and endothelial cell diversification. Cell. 2006;127:1151–1165 [PubMed: 17123592]
16. Valiente-Alandi I, Albo-Castellanos C, Herrero D, Arza E, Garcia-Gomez M, Segovia JC, Capecchi M, Bernad A. Cardiac Bmi1^{+} cells contribute to myocardial renewal in the murine adult heart. Stem Cell Res Ther. 2015;6:205 [PubMed: 26503423]
17. Santini MP, Forte E, Harvey RP, Kovacic JC. Developmental origin and lineage plasticity of endogenous cardiac stem cells. Development. 2016;143:1242–1258 [PubMed: 27095490]
18. Metcalfe C, Kljavin NM, Ybarra R, de Sauvage FJ. Lgr5^{+} stem cells are indispensable for radiation-induced intestinal regeneration. Cell Stem Cell. 2014;14:149–159 [PubMed: 24332836]
19. Schoedel KB, Morcos MN, Zerjatke T, Roeder I, Grinenko T, Voehringer D, Göthert JR, Waskow C, Roers A, Gerbaulet A. The bulk of the hematopoietic stem cell population is dispensable for murine steady-state and stress hematopoiesis. Blood. 2016;128:2285–2296 [PubMed: 27357698]
20. Dovey JS, Zacharek SJ, Kim CF, Lees JA. Bmi1 is critical for lung tumorigenesis and bronchioalveolar stem cell expansion. Proc Natl Acad Sci USA. 2008;105:11857–11862 [PubMed: 18697930]
21. Sangiorgi E, Capecchi MR. Bmi1 is expressed *in vivo* in intestinal stem cells. Nat Genet. 2008;40:915–920 [PubMed: 18536716]

22. Hosen N, Yamane T, Muijtjens M, Pham K, Clarke MF, Weissman IL. Bmi-1-green fluorescent protein-knock-in mice reveal the dynamic regulation of Bmi-1 expression in normal and leukemic hematopoietic cells. Stem Cells. 2007;25:1635–1644 [PubMed: 17395774]
23. Brockschnieder D, Pechmann Y, Sonnenberg-Riethmacher E, Riethmacher D. An improved mouse line for cre-induced cell ablation due to diphtheria toxin a, expressed from the Rosa26 locus. Genesis. 2006;44:322–327 [PubMed: 16791847]
24. Robinet P, Milewicz DM, Cassis LA, Leeper NJ, Lu HS, Smith JD. Consideration of sex differences in design and reporting of experimental arterial pathology studies-statement from ATVB council. Arterioscler Thromb Vasc Biol. 2018;38:292–303 [PubMed: 29301789]
25. Lauden L, Boukouaci W, Borlado LR, López IP, Sepúlveda P, Tamouza R, Charron D, Al-Daccak R. Allogenicity of human cardiac stem/progenitor cells orchestrated by programmed death ligand 1. Circ Res. 2013;112:451–464 [PubMed: 23243206]
26. Torán JL, Aguilar S, López JA, Torroja C, Quintana JA, Santiago C, Abad JL, Gomes-Alves P, Gonzalez A, Bernal JA, Jiménez-Borreguero LJ, Alves PM, R-Borlado L, Vázquez J, Bernad A. CXCL6 is an important paracrine factor in the pro-angiogenic human cardiac progenitor-like cell secretome. Sci Rep. 2017;7:12490 [PubMed: 28970523]
27. Lang RM, Bierig M, Devereux RB, et al. Recommendations for chamber quantification: A report from the american society of echocardiography's guidelines and standards committee and the chamber quantification writing group, developed in conjunction with the european association of echocardiography, a branch of the european society of cardiology. J Am Soc Echocardiogr. 2005;18:1440–1463 [PubMed: 16376782]
28. López-Olañeta MM, Villalba M, Gómez-Salinero JM, Jiménez-Borreguero LJ, Breckenridge R, Ortiz-Sánchez P, García-Pavía P, Ibáñez B, Lara-Pezzi E. Induction of the calcineurin variant cnaβ1 after myocardial infarction reduces post-infarction ventricular remodelling by promoting infarct vascularization. Cardiovasc Res. 2014;102:396–406 [PubMed: 24667850]
29. DeCicco-Skinner KL, Henry GH, Cataisson C, Tabib T, Gwilliam JC, Watson NJ, Bullwinkle EM, Falkenburg L, O'Neill RC, Morin A, Wiest JS. Endothelial cell tube formation assay for the in vitro study of angiogenesis. J Vis Exp. 2014:e51312 [PubMed: 25225985]
30. Fioret BA, Heimfeld JD, Paik DT, Hatzopoulos AK. Endothelial cells contribute to generation of adult ventricular myocytes during cardiac homeostasis. Cell Rep. 2014;8:229–241 [PubMed: 25001281]
31. Chen Q, Zhang H, Liu Y, Adams S, Eilken H, Stehling M, Corada M, Dejana E, Zhou B, Adams RH. Endothelial cells are progenitors of cardiac pericytes and vascular smooth muscle cells. Nat Commun. 2016;7:12422 [PubMed: 27516371]
32. Zeisberg EM, Tarnavski O, Zeisberg M, Dorfman AL, McMullen JR, Gustafsson E, Chandraker A, Yuan X, Pu WT, Roberts AB, Neilson EG, Sayegh MH, Izumo S, Kalluri R. Endothelial-to-mesenchymal transition contributes to cardiac fibrosis. Nat Med. 2007;13:952–961 [PubMed: 17660828]
33. Padrón-Barthe L, Temiño S, Villa del Campo C, Carramolino L, Isern J, Torres M. Clonal analysis identifies hemogenic endothelium as the source of the blood-endothelial common lineage in the mouse embryo. Blood. 2014;124:2523–2532 [PubMed: 25139355]
34. Ito K, Turcotte R, Cui J, Zimmerman SE, Pinho S, Mizoguchi T, Arai F, Runnels JM, Alt C, Teruya-Feldstein J, Mar JC, Singh R, Suda T, Lin CP, Frenette PS. Self-renewal of a purified Tie2^{+} hematopoietic stem cell population relies on mitochondrial clearance. Science. 2016;354:1156–1160 [PubMed: 27738012]
35. Sultana N, Zhang L, Yan J, Chen J, Cai W, Razzaque S, Jeong D, Sheng W, Bu L, Xu M, Huang GY, Hajjar RJ, Zhou B, Moon A, Cai CL. Resident c-Kit^{+} cells in the heart are not cardiac stem cells. Nat Commun. 2015;6:8701 [PubMed: 26515110]
36. van Berlo JH, Kanisicak O, Maillet M, Vagnozzi RJ, Karch J, Lin SC, Middleton RC, Marbán E, Molkentin JD. c-Kit^{+} cells minimally contribute cardiomyocytes to the heart. Nature. 2014;509:337–341 [PubMed: 24805242]
37. Anversa P, Kajstura J, Rota M, Leri A. Regenerating new heart with stem cells. J Clin Invest. 2013;123:62–70 [PubMed: 23281411]

38. Birbrair A, Borges IDT, Gilson Sena IF, Almeida GG, da Silva Meirelles L, Gonçalves R, Mintz A, Delbono O. How plastic are pericytes? Stem Cells Dev. 2017;26:1013–1019 [PubMed: 28490256]
39. Guimarães-Camboa N, Cattaneo P, Sun Y, Moore-Morris T, Gu Y, Dalton ND, Rockenstein E, Masliah E, Peterson KL, Stallcup WB, Chen J, Evans SM. Pericytes of multiple organs do not behave as mesenchymal stem cells in vivo. Cell Stem Cell. 2017;20:345–359 [PubMed: 28111199]
40. Drummond-Barbosa D Stem cells, their niches and the systemic environment: An aging network. Genetics. 2008;180:1787–1797 [PubMed: 19087970]
41. Cochain C, Channon KM, Silvestre JS. Angiogenesis in the infarcted myocardium. Antioxid Redox Signal. 2013;18:1100–1113 [PubMed: 22870932]
42. Talman V, Ruskoaho H. Cardiac fibrosis in myocardial infarction-from repair and remodeling to regeneration. Cell Tissue Res. 2016;365:563–581 [PubMed: 27324127]
43. Bhattacharya R, Mustafi SB, Street M, Dey A, Dwivedi SK. Bmi-1: At the crossroads of physiological and pathological biology. Genes Dis. 2015;2:225–239 [PubMed: 26448339]
44. Balmer GM, Bollini S, Dubé KN, Martinez-Barbera JP, Williams O, Riley PR. Dynamic haematopoietic cell contribution to the developing and adult epicardium. Nat Commun. 2014;5:4054 [PubMed: 24905805]
45. Das S, Red-Horse K. Cellular plasticity in cardiovascular development and disease. Dev Dyn. 2017;246:328–335 [PubMed: 28097739]
46. Robinson SP, Langan-Fahey SM, Johnson DA, Jordan VC. Metabolites, pharmacodynamics, and pharmacokinetics of tamoxifen in rats and mice compared to the breast cancer patient. Drug Metab Dispos. 1991;19:36–43 [PubMed: 1673419]
47. Valiente-Alandi I, Albo-Castellanos C, Herrero D, Sanchez I, Bernad A. Bmi1^{+} cardiac progenitor cells contribute to myocardial repair following acute injury. Stem Cell Res Ther. 2016;7:100 [PubMed: 27472922]
48. Jacobs JJ, Kieboom K, Marino S, DePinho RA, van Lohuizen M. The oncogene and polycomb-group gene Bmi-1 regulates cell proliferation and senescence through the INK4a locus. Nature. 1999;397:164–168 [PubMed: 9923679]
49. Banerjee Mustafi S, Aznar N, Dwivedi SK, Chakraborty PK, Basak R, Mukherjee P, Ghosh P, Bhattacharya R. Mitochondrial Bmi1 maintains bioenergetic homeostasis in cells. FASEB J. 2016;30:4042–4055 [PubMed: 27613804]
50. Jin HJ, Lee HJ, Heo J, Lim J, Kim M, Kim MK, Nam HY, Hong GH, Cho YS, Choi SJ, Kim IG, Shin DM, Kim SW. Senescence-associated MCP-1 secretion is dependent on a decline in BMI1 in human mesenchymal stromal cells. Antioxid Redox Signal. 2016;24:471–485 [PubMed: 26573462]
51. Di Foggia V, Zhang X, Licastro D, Gerli MF, Phadke R, Muntoni F, Mourikis P, Tajbakhsh S, Ellis M, Greaves LC, Taylor RW, Cossu G, Robson LG, Marino S. Bmi1 enhances skeletal muscle regeneration through MT1-mediated oxidative stress protection in a mouse model of dystrophinopathy. J Exp Med. 2014;211:2617–2633 [PubMed: 25452464]
52. Zhou Y, Wang L, Vaseghi HR, Liu Z, Lu R, Alimohamadi S, Yin C, Fu JD, Wang GG, Liu J, Qian L. Bmi1 is a key epigenetic barrier to direct cardiac reprogramming. Cell Stem Cell. 2016;18:382–395 [PubMed: 26942853]
53. Herrero D, Tomé M, Cañón S, Cruz FM, Carmona RM, Fuster E, Roche E, Bernad A. Redox-dependent BMI1 activity drives *in vivo* adult cardiac progenitor cell differentiation. Cell Death Differ. 2018;25:807–820 [PubMed: 29323265]
54. Yan KS, Chia LA, Li X, Ootani A, Su J, Lee JY, Su N, Luo Y, Heilshorn SC, Amieva MR, Sangiorgi E, Capecchi MR, Kuo CJ. The intestinal stem cell markers Bmi1 and Lgr5 identify two functionally distinct populations. Proc Natl Acad Sci USA. 2012;109:466–471 [PubMed: 22190486]
55. Komai Y, Tanaka T, Tokuyama Y, Yanai H, Ohe S, Omachi T, Atsumi N, Yoshida N, Kumano K, Hisha H, Matsuda T, Ueno H. Bmi1 expression in long-term germ stem cells. Sci Rep. 2014;4:6175 [PubMed: 25146451]
56. Biehs B, Hu JK, Strauli NB, Sangiorgi E, Jung H, Heber RP, Ho S, Goodwin AF, Dasen JS, Capecchi MR, Klein OD. Bmi1 represses Ink4a/Arf and Hox genes to regulate stem cells in the rodent incisor. Nat Cell Biol. 2013;15:846–852 [PubMed: 23728424]

57. Shen Q, Goderie SK, Jin L, Karanth N, Sun Y, Abramova N, Vincent P, Pumiglia K, Temple S. Endothelial cells stimulate self-renewal and expand neurogenesis of neural stem cells. Science. 2004;304:1338–1340 [PubMed: 15060285]
58. Kunisaki Y, Bruns I, Scheiermann C, Ahmed J, Pinho S, Zhang D, Mizoguchi T, Wei Q, Lucas D, Ito K, Mar JC, Bergman A, Frenette PS. Arteriolar niches maintain haematopoietic stem cell quiescence. Nature. 2013;502:637–643 [PubMed: 24107994]
59. Bergmann O, Zdunek S, Felker A, et al. Dynamics of cell generation and turnover in the human heart. Cell. 2015;161:1566–1575 [PubMed: 26073943]
60. Bunting KD. Abc transporters as phenotypic markers and functional regulators of stem cells. Stem Cells. 2002;20:11–20 [PubMed: 11796918]
61. Sarkar A, Hochedlinger K. The Sox family of transcription factors: Versatile regulators of stem and progenitor cell fate. Cell Stem Cell. 2013;12:15–30 [PubMed: 23290134]
62. Liu J, Willet SG, Bankaitis ED, Xu Y, Wright CV, Gu G. Non-parallel recombination limits cre-loxp-based reporters as precise indicators of conditional genetic manipulation. Genesis. 2013;51:436–442 [PubMed: 23441020]
63. McNally EM, Golbus JR, Puckelwartz MJ. Genetic mutations and mechanisms in dilated cardiomyopathy. J Clin Invest. 2013;123:19–26 [PubMed: 23281406]
64. Wang J, Hoshijima M, Lam J, Zhou Z, Jokiel A, Dalton ND, Hultenby K, Ruiz-Lozano P, Ross J, Tryggvason K, Chien KR. Cardiomyopathy associated with microcirculation dysfunction in Laminin α4 chain-deficient mice. J Biol Chem. 2006;281:213–220 [PubMed: 16204254]
65. Shiojima I, Sato K, Izumiya Y, Schiekofer S, Ito M, Liao R, Colucci WS, Walsh K. Disruption of coordinated cardiac hypertrophy and angiogenesis contributes to the transition to heart failure. J Clin Invest. 2005;115:2108–2118 [PubMed: 16075055]
66. Kivelä R, Bry M, Robciuc MR, et al. VEGF-B-induced vascular growth leads to metabolic reprogramming and ischemia resistance in the heart. EMBO Mol Med. 2014;6:307–321 [PubMed: 24448490]
67. Asahara T, Murohara T, Sullivan A, Silver M, van der Zee R, Li T, Witzenbichler B, Schatteman G, Isner JM. Isolation of putative progenitor endothelial cells for angiogenesis. Science. 1997;275:964–967 [PubMed: 9020076]
68. Ubil E, Duan J, Pillai IC, Rosa-Garrido M, Wu Y, Bargiacchi F, Lu Y, Stanbouly S, Huang J, Rojas M, Vondriska TM, Stefani E, Deb A. Mesenchymal-endothelial transition contributes to cardiac neovascularization. Nature. 2014;514:585–590 [PubMed: 25317562]
69. He L, Huang X, Kanisicak O, et al. Preexisting endothelial cells mediate cardiac neovascularization after injury. J Clin Invest. 2017;127:2968–2981 [PubMed: 28650345]

HIGHLIGHTS

- $Sca1^{+}Bmi1^{+}$ progenitor cells are dispensable for cardiac homeostasis in adult mice
- $Sca1^{+}Bmi1^{+}$ progenitor cells are important for infarct-induced neovascularization
- $Sca1^{+}Bmi1^{+}CD31^{+}$ progenitor subpopulation is highly prone to endothelial cell generation

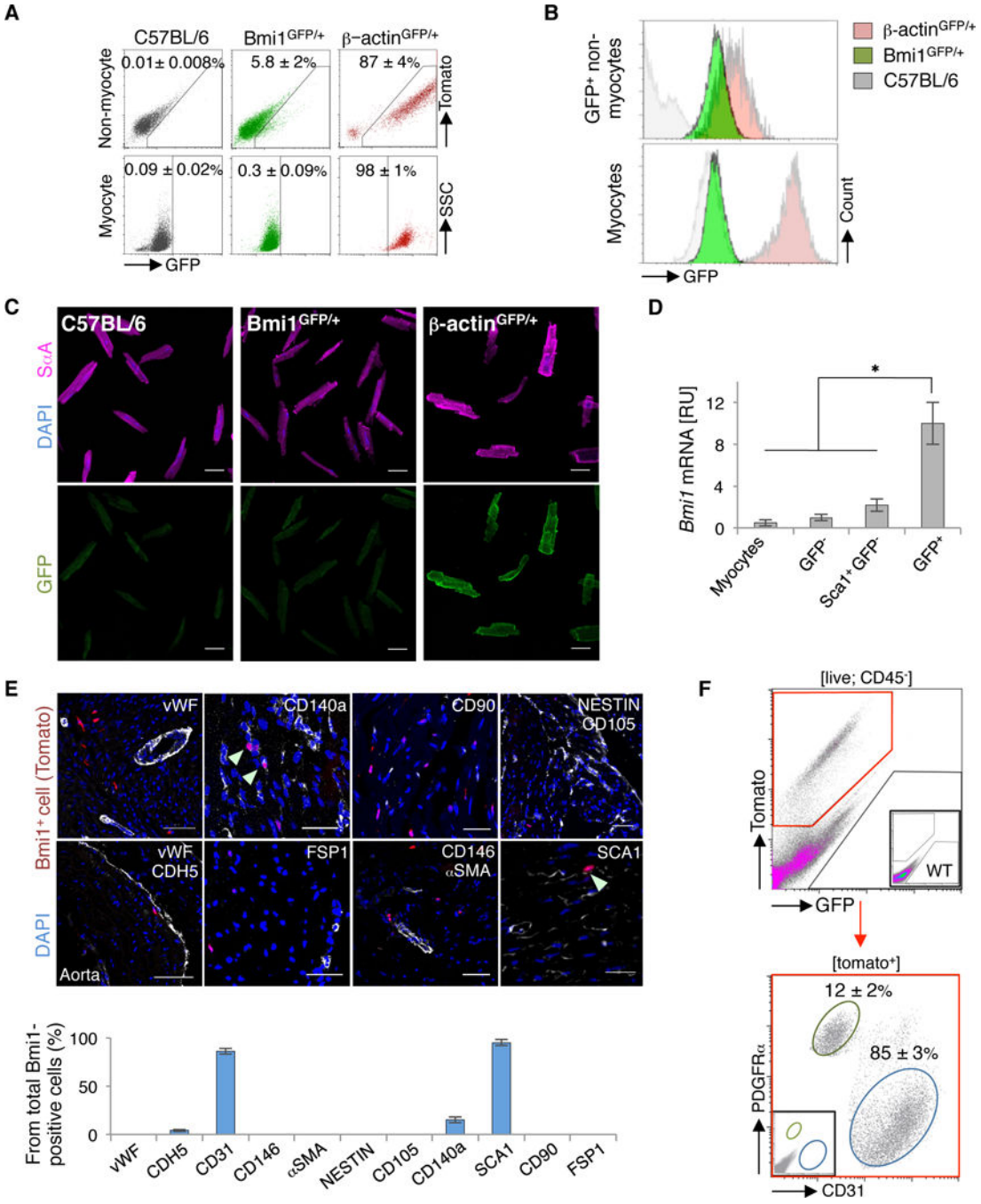

Figure 1.

BMI1 expression identifies a mixture of endothelial- and mesenchymal-related non-myocyte cells in the adult heart. **A,** Representative FACS plots of non-myocyte cells and cardiomyocytes from adult C57BL/6 (grey), Bmi1$^{GFP/+}$ (green) and β-actin$^{GFP/+}$ mice (red) (n = 4). **B,** Histograms of GFP levels of indicated cardiac cell populations from adult C57BL/6 (grey), Bmi1$^{GFP/+}$ (green) and β-actin$^{GFP/+}$ mice (red) (n = 4). **C,** Representative immunocytochemistry of cardiomyocytes from adult C57BL/6, Bmi1$^{GFP/+}$ and β-actin$^{GFP/+}$ mice. C57BL/6 cardiomyocytes show GFP background. **D,** *In vivo Bmi1* expression of

indicated cardiac cell populations from Bmi1$^{GFP/+}$ mice (n = 4). ∗ p <0.05; Kruskall-Wallis ANOVA test. [RU], relative units. **E,** Top: Immunohistochemical characterization of Bmi1^{+} cardiac cells in adult Bmi1$^{CreERT/+}$Rosa26$^{Tomato/+}$ heart cryosections stained with indicated markers at 5 days post-Tx induction. Arrowheads, double-positive cells. Bottom: Immunohistochemical quantification of surface cell marker expression in the Bmi1^{+} cardiac cell population (n = 3). Bars, 50 μm. **F,** Representative FACS plot of CD31 and PDGFRα surface marker expression in Bmi1^{+} cardiac cells from Bmi1$^{CreERT/+}$Rosa26$^{Tomato/+}$ mice, 5 days post-Tx induction (n = 4). Data shown as mean ± SEM.

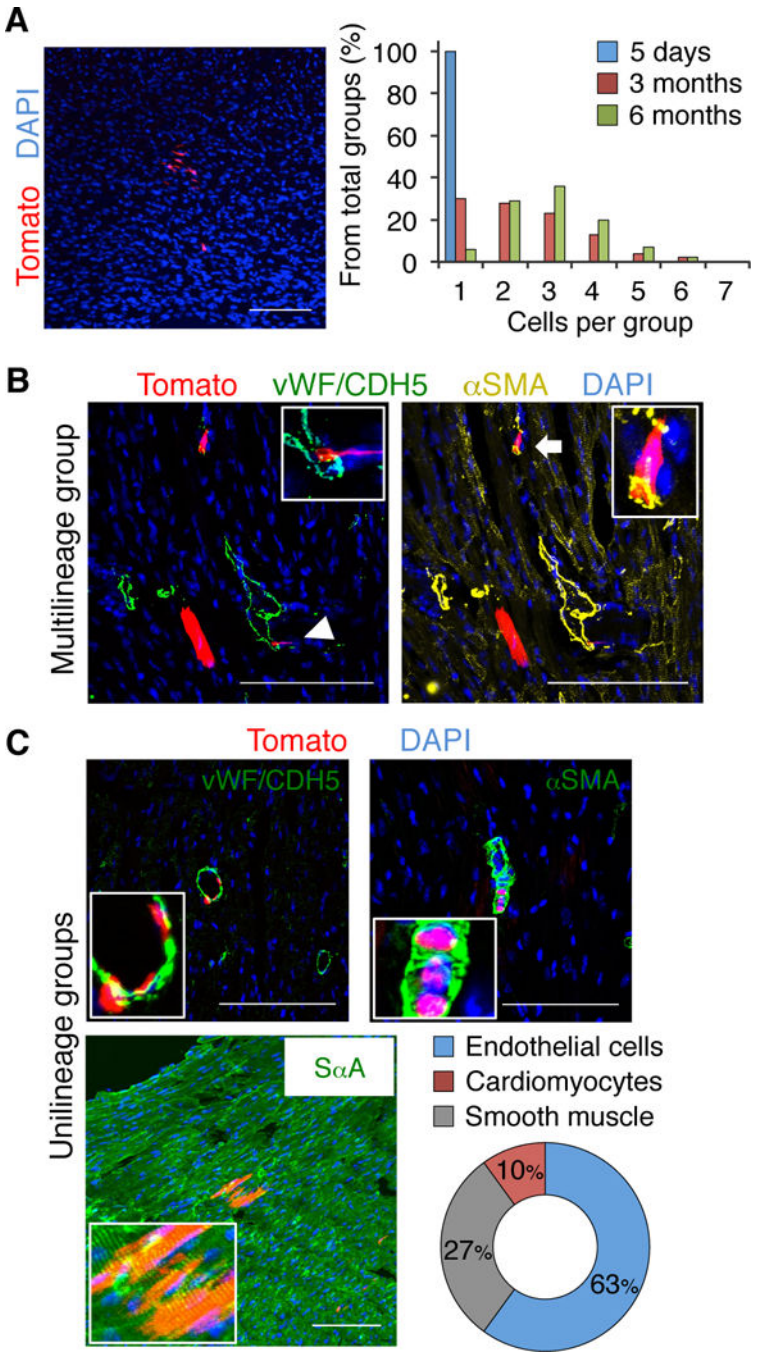

Figure 2.

Bmi1^{+} cardiac progenitor cells have *in vivo* differentiation capacity with limited multilineage potential. **A,** Left: Large Bmi1-derived cell group (Tomato^{+}) in Bmi1$^{CreERT/+}$Rosa26$^{Tomato/+}$ heart, 6 months post-low Tx induction. Right: Size quantification of Bmi1-derived cell group in cryosections at 5 days, 3 and 6 months post-low Tx induction (n = 3). **B** and **C**, Representative views of a rare multilineage Bmi1-derived cell group (composed of cardiomyocyte, endothelial cell (arrowhead) and smooth muscle (arrow)) (**B**) and more frequent unilineage groups (**C**) in Bmi1$^{CreERT/+}$Rosa26$^{Tomato/+}$

hearts, 6 months post-low Tx induction, with cell type quantification ($n = 3$). *Insets*, Bmi1-derived differentiated cells (5x magnification). Bars, 100 μm. Data shown as mean ± SEM.

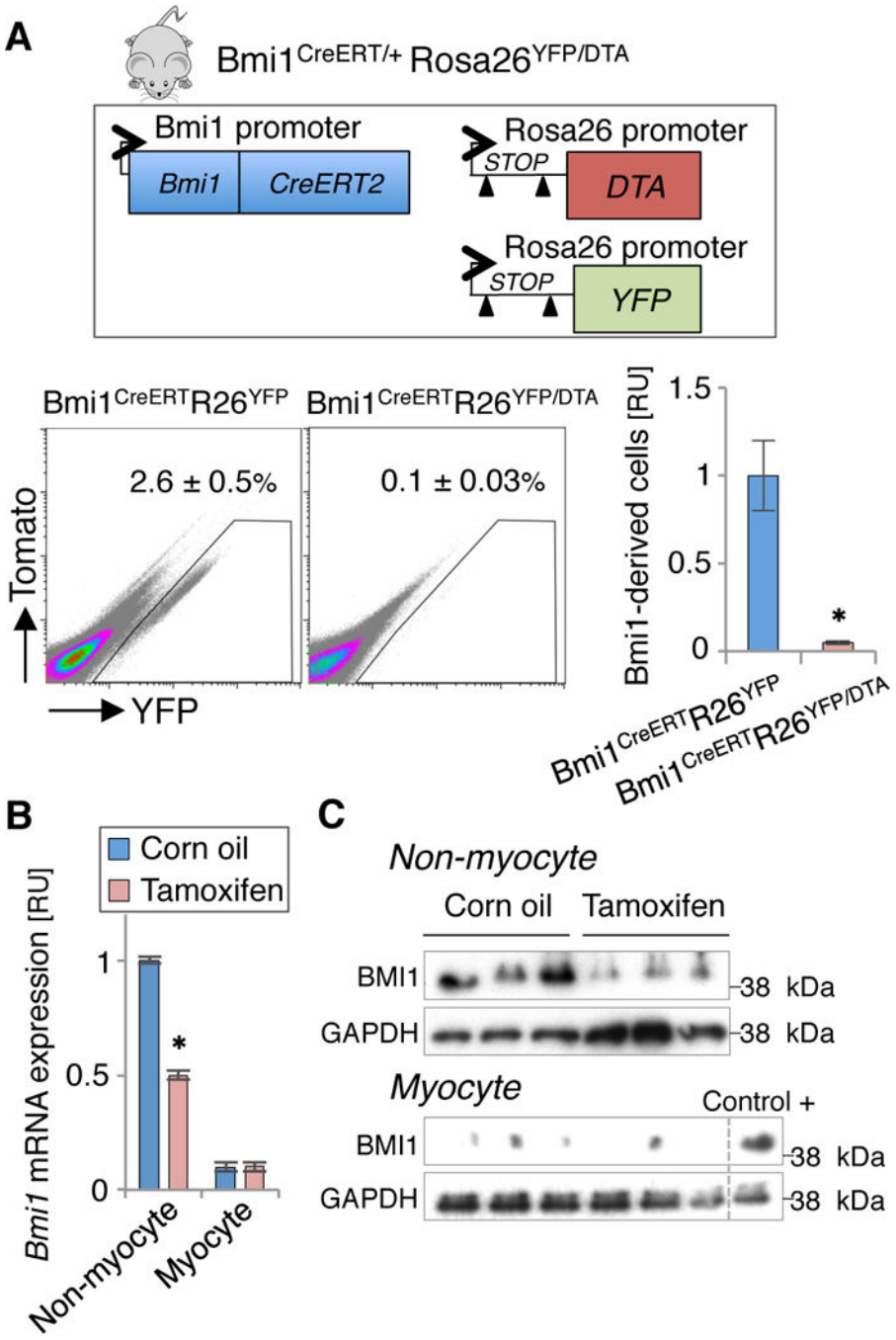

Figure 3.

Conditional diphtheria toxin A (DTA) expression induces efficient ablation of adult Bmi1^{+} cardiac progenitor cells. **A,** Comparative FACS analyses of Bmi1^{+} cardiac progenitor cells (YFP^{+}) from bigenic Bmi1$^{CreERT/+}$Rosa26$^{YFP/+}$ and trigenic Bmi1$^{CreERT/+}$Rosa26$^{YFP/DTA}$ mouse hearts, 5 days post-Tx induction (n = 4). ∗ p <0.05; Mann-Whitney rank sum test. **B** and **C,** Tx treatment induced downregulation of *Bmi1* expression only in the non-myocyte fraction in Bmi1$^{CreERT/+}$Rosa26$^{YFP/DTA}$ hearts 5 days post Tx induction, measured by RT-

qPCR (**B**) and western blot (**C**) ($n \geq 3$). Control+: non-myocyte cells as positive control for BMI1. ∗ $p < 0.05$; Mann-Whitney rank sum test. Data shown as mean ± SEM.

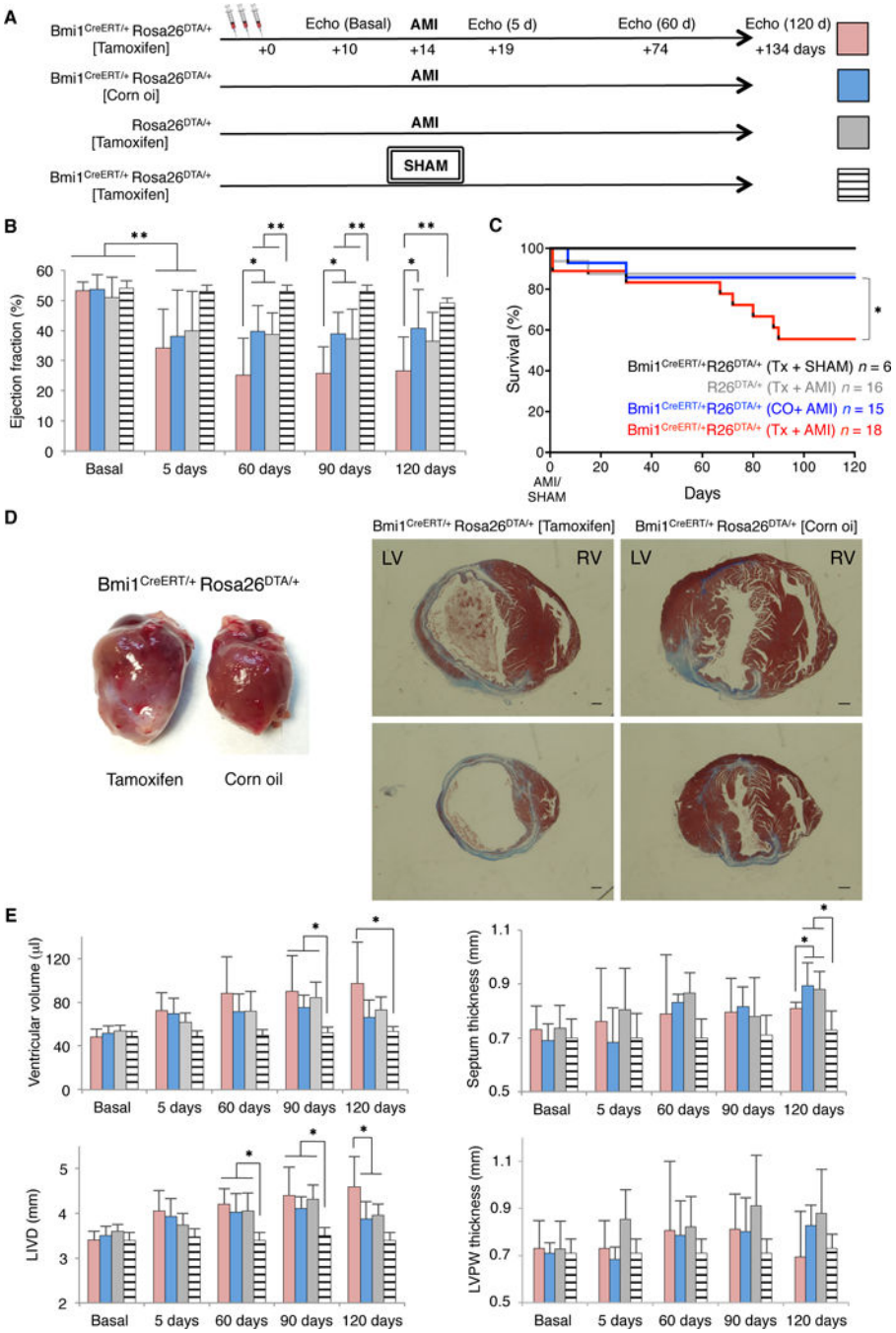

Figure 4.

Bmi1^{+} progenitor cells are necessary for natural cardiac remodeling after acute myocardial infarction (AMI). **A,** Timeline echocardiography analyses to evaluate the effects of induced heart injury on the different transgenic mouse lines. Tx induction (d0); AMI (d14). **B,** Trans-thoracic M-mode echocardiography of ejection fraction from infarcted transgenic mice before (basal) and at indicated times after AMI. ∗ p <0.05, ∗∗ p <0.005; one-way ANOVA with Tukey's post-hoc test. **C,** Kaplan-Meier survival curves for the indicated groups of mice. **D,** Gross cardiac phenotype (left) and representative Masson's trichrome-stained

transverse paraffin sections (right) of Tx- and vehicle-treated Bmi1$^{CreERT/+}$Rosa26$^{DTA/+}$ hearts, 4 months after AMI. Bars, 1 mm. **E,** Trans-thoracic M-mode echocardiography of physiological parameters from infarcted transgenic mice before (basal) and at indicated times after AMI. ∗ $p < 0.05$; one-way ANOVA with Tukey's post-hoc test. (B,C,E,): Number of mice (*n*) per group is indicated in panel C. LIVD: Left internal ventricular diameter, LVPW: Left ventricular posterior wall. Data shown as mean ± SEM.

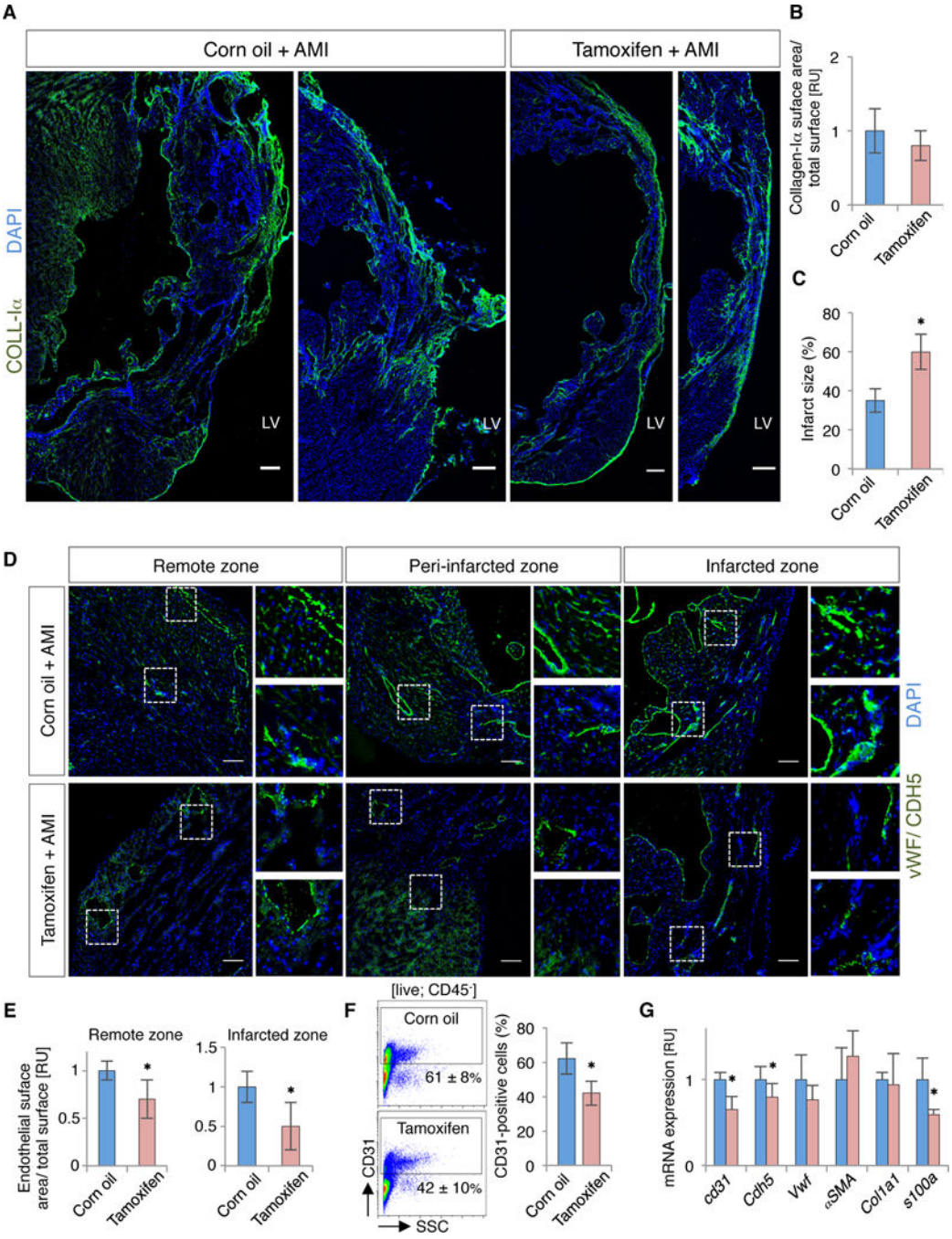

Figure 5.

Bmi1^{+} cell-deficient hearts show impaired angiogenesis and increased scar size after AMI. **A,** Representative cryosections of cardiac fibrosis (collagen-Iα^{+}; coll-Iα) from vehicle- and Tx-treated Bmi1$^{CreERT/+}$Rosa26$^{DTA/+}$ hearts, 4 months after AMI. Bars, 100 μm. **B** and **C,** Quantification of collagen-Iα deposition (**B**) and LV scar size (**C**) on cryosections of vehicle- and Tx-treated Bmi1$^{CreERT/+}$Rosa26$^{DTA/+}$ mice, 4 months after AMI (n = 5). **D** and **E,** Representative cryosections (**D**) and quantification (**E**) of cardiac vasculature (vWF/ CDH5) from vehicle- and Tx-treated Bmi1$^{CreERT/+}$Rosa26$^{DTA/+}$ hearts, 4 months after AMI

(*n* = 5). Bars, 50 μm. **F,** Representative FACS plot (left) and quantification (right) of $CD31^+$ cardiac endothelial cells from vehicle- and Tx-treated $Bmi1^{CreERT/+}Rosa26^{DTA/+}$ hearts, 2 months after AMI (*n* = 4). Isotype control in Figure 6D. **G,** $Bmi1^+$ cell-deficient hearts (red) showed decreased endothelial-related gene expression compared to controls (blue) at 4 months after AMI, measured by RT-qPCR (*n* = 4). Analyses: ∗ $p < 0.05$; Mann-Whitney rank sum test. Data shown as mean ± SEM.

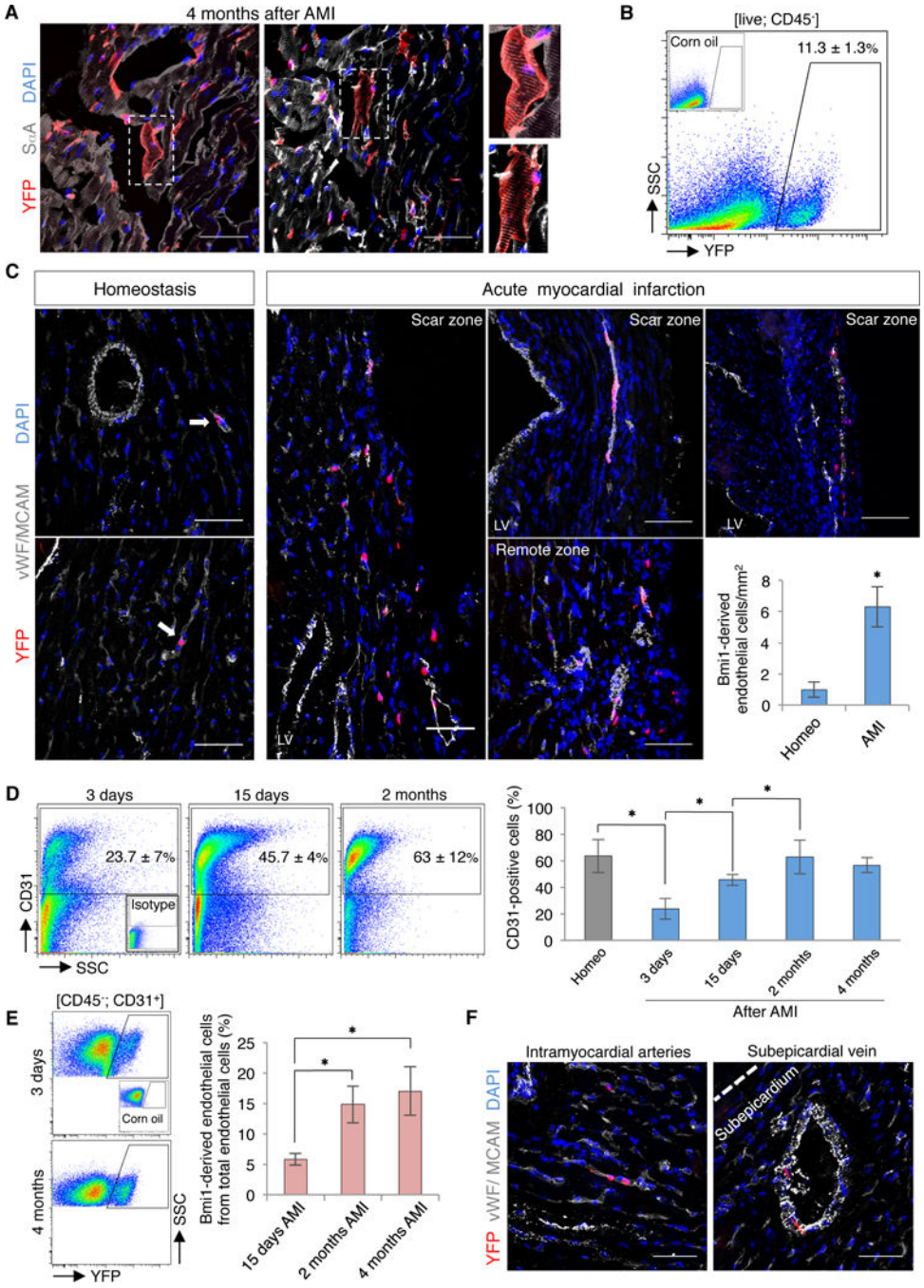

Figure 6.

Bmi1^{+} progenitor cells are key contributors to cardiac vasculature after AMI. **A,** Representative cryosections of Bmi1-derived cells (YFP^{+}) in remote areas of Bmi1$^{CreERT/+}$Rosa26$^{YFP/+}$ hearts, 4 months after AMI. *Insets*, Bmi1-derived cardiomyocytes (2x magnification). **B,** FACS analysis of non-myocyte heart fraction from Bmi1$^{CreERT/+}$Rosa26$^{YFP/+}$ mice showed a large percentage of Bmi1-derived cells, 4 months after AMI (n = 5). **C,** Representative cryosections and quantification of Bmi1-derived endothelial cells (vWF/CDH5^{+}) in Bmi1$^{CreERT/+}$Rosa26$^{YFP/+}$ hearts at 4 months after AMI

vs. age-matched controls (homeo) ($n = 5$). Arrows: Bmi1-derived endothelial cells. ∗ p <0.05; Mann-Whitney rank sum test. **D,** Representative FACS plots (left) and quantification (right) of cardiac endothelial cells ($CD31^+$) in homeostasis and at 3 and 15 days, 2 and 4 months after AMI in $Bmi1^{CreERT/+}Rosa26^{YFP/+}$ hearts ($n \geq 3$). ∗ p <0.05; Kruskall-Wallis ANOVA test. **E,** Representative FACS plots (left) and quantification (right) of Bmi1-derived endothelial cells in $Bmi1^{CreERT/+}Rosa26^{YFP/+}$ hearts during the infarct-induced angiogenic response ($n \geq 4$). ∗ p <0.05; Kruskall-Wallis ANOVA test. **F,** Representative views of Bmi1-derived endothelial cells ($vWF/CDH5^+$) in intramyocardial arteries and subepicardial veins of $Bmi1^{CreERT/+}Rosa26^{YFP/+}$ hearts, 4 months after AMI. Bars, 50 μm. Data shown as mean ± SEM.